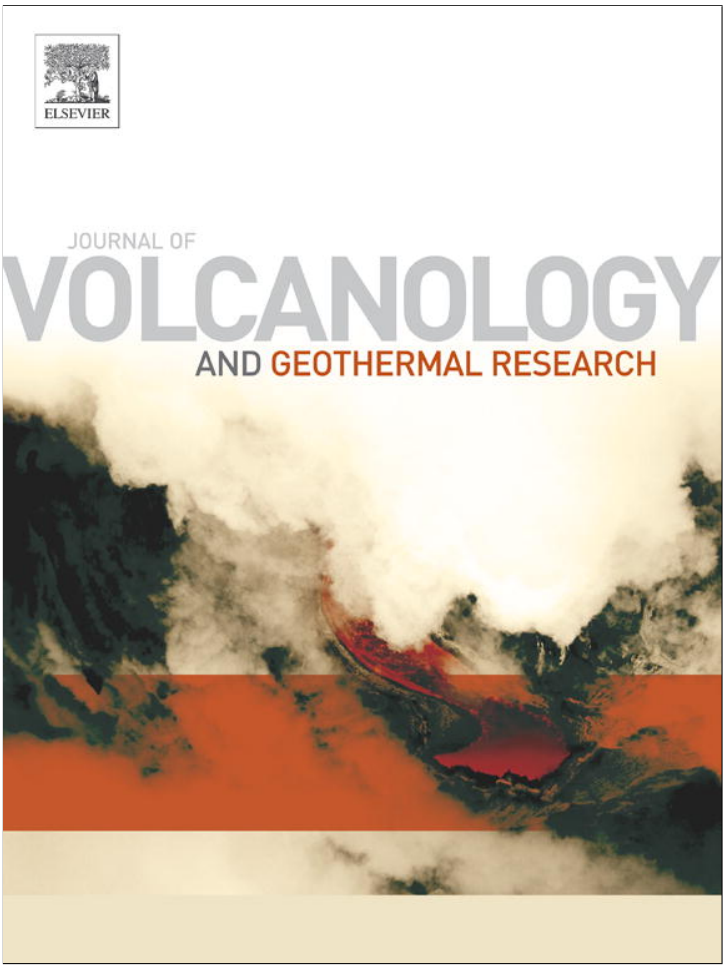

(This is a sample cover image for this issue. The actual cover is not yet available at this time.)

Journal of Volcanology and Geothermal Research 255 (2013) 90–97

Contents lists available at SciVerse ScienceDirect

Journal of Volcanology and Geothermal Research

journal homepage: www.elsevier.com/locate/jvolgeores

Somma-Vesuvius ground deformation over the last glacial cycle

Aldo Marturano [a,*], Giuseppe Aiello [b], Diana Barra [b,a]

[a] Istituto Nazionale di Geofisica e Vulcanologia, sez. Osservatorio Vesuviano, via Diocleziano 328, 80124 Napoli, Italy
[b] Dipartimento di Scienze della Terra, Università di Napoli Federico II, Largo San Marcellino 10, 80136 Napoli, Italy

ARTICLE INFO

Article history:
Received 4 July 2012
Accepted 13 February 2013
Available online 21 February 2013

Keywords:
Somma-Vesuvius
Palaeoecology
Crustal deformation
Sea-level change correlation

ABSTRACT

Vertical ground movements at Somma-Vesuvius during the last glacial cycle have been inferred from micropalaeontological and petrochemical analyses of rock samples from boreholes drilled at the archaeological sites of Herculaneum and Pompeii as well as on the apron of the volcano and the adjacent Sebeto and Sarno Valleys. Opposing movements occurred during the periods preceding and following the Last Glacial Maximum (LGM). The uplift began 20 ka ago with marine deposits rising several tens of metres up to 25 m a.s.l., recovering previous subsidence which occurred during the Late glacial period, suggesting a strict connection between volcano–tectonic and glacial cycles. Here we present the analysis of deposits predating the LGM, which confirms subsidence of the Campanian Plain where Mt. Somma-Vesuvius is located, shows variable surface loading effects and highlights the volcano–tectonic stages experienced by the volcano. The self-balancing mechanism of the volcanic system, evolving towards an explosive, subaerial activity 60 ka ago, is testified to by a large ground oscillation in phase with sea level change during the last glacial cycle.

1. Introduction

Somma–Vesuvius is located on the eastern margin of the Campanian Plain graben (Southern Italy) (Fig. 1), which formed a part of the extensive tectonic activity related to the opening of the Tyrrhenian Sea and widespread volcanism (Patacca et al., 1990). The Campanian Plain is considered to have subsided during the Plio-Quaternary age (e.g., Ippolito et al., 1973). Although volcanism in the area may have started around 300–400 ka, the volcano emerged as Mt. Somma during the late glaciation (Di Renzo et al., 2007). The products of the activity that formed the Somma stratovolcano consist of a pile of lava flow spatter and scoria deposits reflecting dominantly effusive activity (Santacroce, 1987).

Major plinian eruptions are recognised as having occurred only in the last 40 ka: "Codola" (C, ~33 ka), "Pomici di Base" (B, 22 ka), "Mercato" (M, 8.9 ka), "Avellino" (A, 4.3 ka) and AD 79 Pompeii eruption (P). The recent cone, Vesuvius, grew within the caldera after the AD 79 eruption. These events alternated with less explosive sub-plinian eruptions (e.g., the ~19 ka "Pomici Verdoline", the AD 412 "Pollena" and AD 1631 "Villa Inglese") and quiescent phases, commonly ascribed to a somewhat cyclic alternation between periods of obstructed conduit and periods of open conduit conditions (Santacroce et al., 2008) (Fig. 2).

A deformation history of the Somma-Vesuvius volcano since the Last Glacial Maximum (LGM, 20 ka) was recently reconstructed by utilising archaeological, micropalaeontological, archaeometric and petrochemical analyses of samples from trenches and boreholes at the archaeological sites of Herculaneum and Pompeii and in the adjacent Sebeto and Sarno Valleys (Marturano et al., 2009, 2011, 2012). The data depict a framework of large uplift followed by relative stability. Ground deformation appears to have taken place over several ka at Somma-Vesuvius and uplift was seemingly in progress a few ka after the beginning of the interglacial phase (~20 ka). This uplift suggests that the volcanic component prevailed over the long-term subsidence of the entire Campanian Plain.

In particular, early data record long-term deformation (at the rate of ~5 mm/yr) at Pompeii, the Pompeii apron and Sarno Valley (i.e., southeast of Mt. Somma-Vesuvius). Despite incomplete field sampling, Marturano et al. (2011) supposed that such movements extended over the whole Somma-Vesuvius area and that the uplift was of volcanic origin.

The ground deformation was simulated by considering a dislocation model, a horizontal sheet, based on the formulas by Okada (1992) for a homogeneous half space. The source, 20–25 km deep, corresponding to the depth of the low velocity zone (e.g., Panza et al., 2007), was centred along the axis of the summit caldera of the volcano. The source was assumed to be as large as the base of the volcano (20 km) and the parameters were calibrated to obtain a vertical rate of 5 mm/year ~10 km away from the axis, and taking into account estimated values of the magma supply rate (Joron et al., 1987; Cioni et al., 2003).

The uplift at Herculaneum appears to have occurred at a rate and during a time lapse comparable with that recorded at Pompeii and its apron (Marturano et al., 2012). Furthermore, ground deformation that included the Sebeto–Volla Valley on the northwestern side occurred in similar fashion to that of the Sarno Valley in the

* Corresponding author. Tel.: +39 081 6108439; fax: +39 081 6100811.
E-mail address: aldo.marturano@ov.ingv.it (A. Marturano).

0377-0273/$ – see front matter © 2013 Elsevier B.V. All rights reserved.
http://dx.doi.org/10.1016/j.jvolgeores.2013.02.007

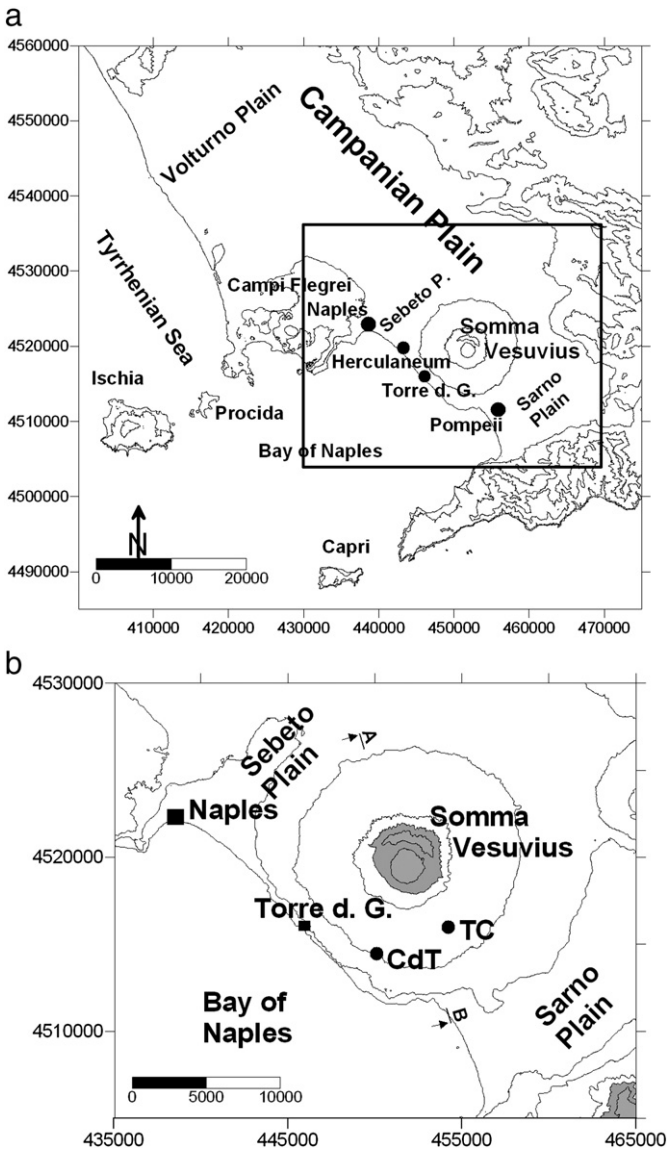

Fig. 1. a) Campanian Plain and Somma-Vesuvius. b) Sketch map of the Somma-Vesuvius. CdT and Tc are the locations of Camaldoli della Torre and Trecase boreholes respectively.

southeast. All these results portray a framework of synchronous ground movements for the whole Somma-Vesuvius edifice and the complete deformation dataset appears possibly to follow an exponential law. Therefore, long-term volcano deformation at Somma-Vesuvius was modelled assuming Maxwell viscoelastic behaviour for the lower crust below the volcano (Marturano et al., 2012), and, in order to compare the results, the source of strain of the new model was located at a depth of $h = 20$ km, as proposed in the elastic model of Marturano et al. (2011). The source, within the lower crust, was modelled by a spherical pressure source of 5 km of radius (R1), surrounded by a concentric spherical Maxwell viscoelastic shell of 10 km radius (R2), embedded within an elastic full space. R1 and R2 had the same origin, coinciding with the centre of the magma body. The shear modulus μ was assumed to be $5 \cdot 10^9$ Pa (e.g., Bonafede et al., 1986), and the viscosity $\eta = 10^{18}$–10^{19} Pa·s (typical for the lower crust of the Somma-Vesuvius area as well as for volcanic regions worldwide; e.g., Jull and McKenzie, 1996; Borgia et al., 2005; Dalla Via et al., 2005; Nooner et al., 2009; Karlstrom et al., 2010). The test showed that the vertical deformation ($\Delta h \approx 80$ m) recorded at ~10 km around Somma-Vesuvius could be obtained by a linearly increasing pressure up to ~250 MPa, a value lower than the lithostatic pressure ($P_{litho} = h \cdot \rho \cdot g \approx 500$ MPa; $\rho = 2600$ kg/m^3) at source depth. The pressure increase (ΔP) was associated with an increase in the spherical source volume ($\Delta V = \sim 20$ km^3) according to $\Delta P = \mu \cdot \Delta V / (\pi \cdot R^3)$, one order of magnitude lower than the value obtained by the elastic model (Marturano et al., 2011). Even if a critical overpressure lower than 100 MPa inferred in the shallow system cannot be directly applied to rupturing of deep chambers (e.g., Karlstrom et al., 2010), the calculated overpressure may appear too high. At this point it should be stressed that the size of the sources (R1 and R2) cannot be uniquely determined from geodetic data alone given the trade-off between source dimension and source pressure. In comparison, if R1 = 10 km, R2 = 20 km and h = 30 km (Moho depth), the pressure and volume increase is $\Delta P = 60$ MPa and $\Delta V = 40$ km^3 respectively. The best-fit curve for this model is in Fig. 3. In the same figure is also reported the best fit (straight line) related to the expansion of a point source 30 km deep embedded in a homogeneous half space producing a source volume variation of about 300 km^3. In order to obtain a pressure increase the same as that of the viscoelastic model, a source radius of 20 km has to be considered.

A widely used statistic for evaluating goodness of the fit of a model to N data is χ^2, defined as $\sum_i [(d_i^o - d_i^p)/\sigma i]^2$ where d_i^p is the predicted value, d_i^o and σ_i are the observed value and the error assigned to the observed datum (Gordon et al., 1987). The reduced chi-square, χ^2_ν, defined as the ratio of χ^2_ν to the number of degrees of freedom (ν), was utilised. Values of χ^2_ν much greater than 1 suggest poor fits of the model to the data, whereas values of χ^2_ν near 1 suggest good fits of the model to the data. The values obtained for the elastic rheology and viscoelastic model are $\chi^2_\nu = 4.3$ and 4.2 respectively, suggesting comparable fits of both models to the data. To compare variances of distributions the F-ratio statistical test was used. Results of the Fisher's exact test show that, although the norm of residuals is lower for the exponential fit, the variance ratio does not allow distinction between the two models. Indeed, the value obtained is

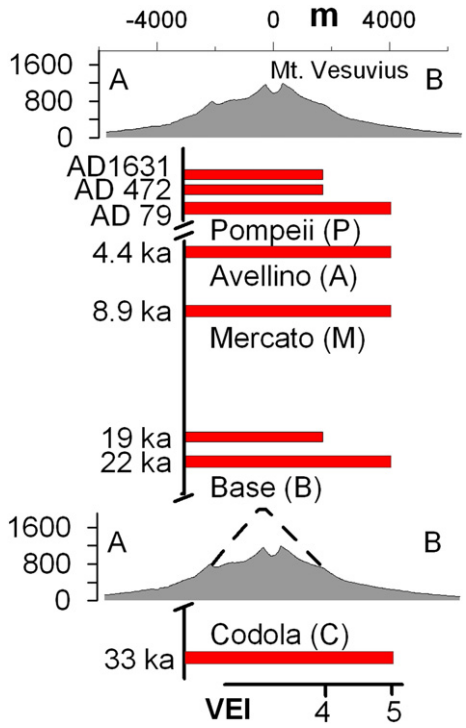

Fig. 2. Chronogram of Somma-Vesuvius activity. Plinian and sub-plinian eruptions (Volcanic Explosivity Index, VEI 4–5) are reported (scale on the bottom). In the two schematic cross sections (A–B in Fig. 1b) the grey areas represent the present Somma-Vesuvius while the dashed line shows the contour of Mt. Somma before the calderisation by B, M, A, P plinian eruptions.

below the discrimination threshold. In the following, as representative, we will utilise the curve related to the viscoelastic model.

The reconstructed pressure history (Fig. 3) indicates a two-stage evolution, reflecting two phases: an early phase of pressure increase, in which the entire volcanic edifice is uplifted by tens of metres incorporating tens of km^3 of new magma in a period of low eruptive documented activity; a late phase in which the volcano appears to have settled into a new equilibrium during which pressure remains constant. Three plinian eruptions occurred at 8.9 (M), 4.3 (A) and 1.9 ka (P) (triangles in Fig. 3) after intervals of variable length. Studies of ground deformations of plinian eruptions, like the last one in AD 79, suggest a source of strain at a depth of ~8 km (Marturano, 2008). When taken together, these observations constrain our proposed model of two vertically stacked sources: one 20–30 km deep, and the shallower source in the middle crust (10–8 km), corresponding to a difference in pressure of 200–250 MPa.

Extensive geophysical and petrological studies have helped to constrain the nature of the crust below Somma Vesuvius (e.g., Zollo et al., 1998; De Natale et al., 2006; Nunziata et al., 2006). These studies indicate a shallow high-rigidity anomaly clustering seismicity and possibly small shallow magma pockets, a mid-crustal ductile boundary and deeper decrease in the shear wave velocities, suggesting the presence of partially molten material. As in the models, the top of the system at 10–8 km coincides with the seismic attenuation imaged by geophysical surveys and confining with seismicity recorded at Vesuvius since 1944 at depths shallower than 6 km; the deep source (20–30 km) is fixed close to the lower crust–mantle boundary characterised by a lower shear wave velocity. Phase relationships suggest equilibration pressure (P≈200 MPa) for the last three plinian eruptions, indicating stable mid-crustal magma storage around 8 km, and pressure of 300–500 MPa for the B eruption, corresponding to deeper storage (Scaillet et al., 2008).

An important difference between the two models proposed relates to the extent of the source and the volume of mass movement. In the elastic model the source extends for a distance at least five times larger than the base radius of the Somma-Vesuvius, presupposing significant doming also below adjacent volcanic areas (e.g., Campi Flegrei Volcanic Field). On the contrary, the viscoelastic model considers one order of magnitude smaller movement of mass in an expanding local source confined below the Somma-Vesuvius.

In conclusion, the models proposed suggest that in the long term Mt. Somma-Vesuvius acts as a single structural element in response to deep (lower crust–mantle boundary) magma movements. Also, the model assumes that, in the last 20 ka, the uplift of volcanic origin has overcome the general subsidence framework of the Campanian Plain.

However, our knowledge of how the volcano works must expand upon the period prior to the LGM in order to examine how the system responds to seemingly different external conditions. The present study is based on a multidisciplinary approach undertaken to characterise the palaeo-environmental record recovered in the levels that predate the LGM so as to analyse the ground movement that occurred before the ascertained uplift recorded after the LGM. The studied sequence includes deposits predating the Campanian Ignimbrite (CI, 39 ka) from the Camaldoli della Torre (CdT) borehole drilled on the S of the Somma-Vesuvius caldera.

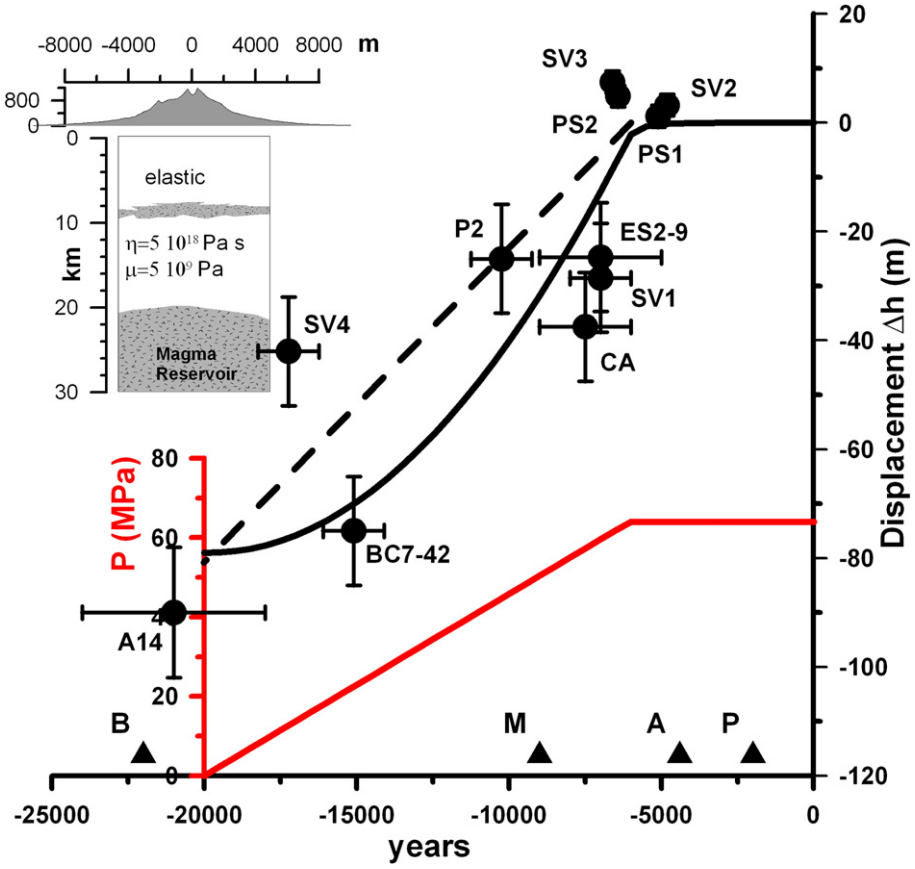

Fig. 3. Ground uplift history (scale on the right) at Somma-Vesuvius in the last 20 kyr as reconstructed applying the viscoelastic (continuous line) and elastic (dashed line) models: $|\Delta h_{max}| = 80$ m. Pressure history (scale on the left) for the viscoelastic (R1 = 10 km, R2 = 20 km, h = 30 km) and elastic models (h = 30 km). The circles with error bars specify the displacements for archaeological sites of Herculaneum (ES2-9, P2) and Pompeii (CA) and in the adjacent Sebeto (SV1-2-3-4) and Sarno (PS1-2, BC7-42, A14) Valleys (Marturano et al., 2012). The triangles represent the plinian eruptions. Inset: viscoelastic model.

2. Microfossil remains and palaeoenvironmental interpretation

A 240 m deep borehole was drilled at Camaldoli della Torre (CdT) on the southern slope of Mt. Vesuvius, close to the town of Torre del Greco (Fig. 1b), at ~5 km from the centre and at ~3 km from the rim of the summit caldera of the volcano.

The well reached a maximum depth of 121.6 m b.s.l., enabling detailed stratigraphic, sedimentological, petrological and geochemical analyses by continuous coring (Di Renzo et al., 2007). The deep stratigraphic sequence (Fig. 4) includes 10 units separated by palaeosoils and lacustrine deposits (P and d in Fig. 4) underlying the CI, an explosive eruption that covered the entire Campanian Plain and the bordering limestone terrains with a layer several metres thick, and dispersed 250–300 km^3 of ash over $7.7 \cdot 10^6$ km^2 (Fedele et al., 2008). Dated 39 ka (De Vivo et al., 2001) it is the dominant event of the region, having released 180–280 km^3 (DRE) of trachytic rocks (Costa et al., 2012).

Nine samples (Table 1) were collected from selected sedimentary layers belonging to the CdT core, with the aim of defining the palaeoecology of the section by means of microfossil remains. Samples (200 g dry weight) were disaggregated, washed with water through 230 and 120 mesh sieves (respectively, 63 and 125 μm). Both fractions were analysed, fossil remains being picked from the coarsest fraction.

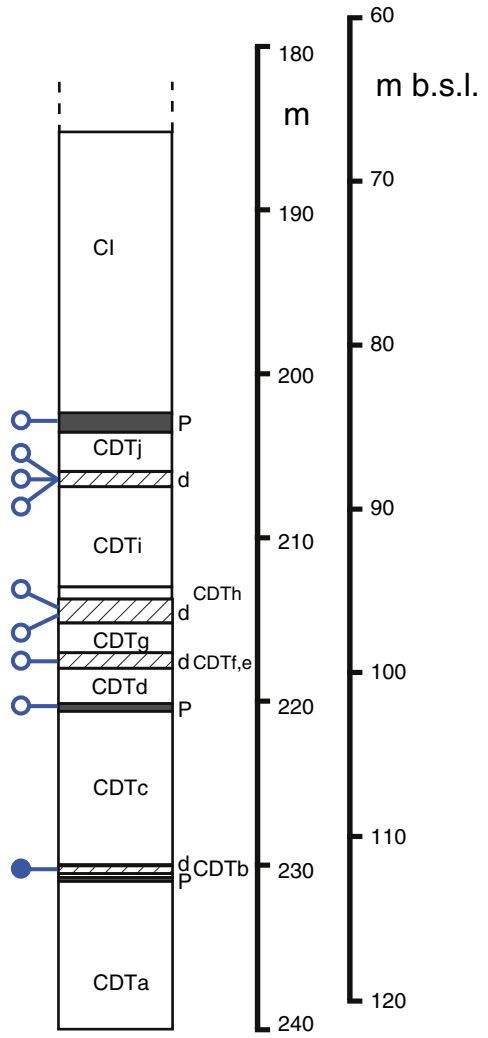

Fig. 4. Stratigraphy (deeper part) of the Camaldoli della Torre (CdT) borehole (simplified from Di Renzo et al., 2007). On the right the borehole depth and below sea level elevation in metres (m b.s.l.), on the left the stratigraphic height of the samples utilised for fossiliferous analyses. Full circle: fossiliferous sample.

Table 1
CdT 230.80–230.90. Abundance of ostracod species in the sample CDT 230.80–230.90; alv = adult left valves; arv = adult right valves; jlv = juvenile left valves; jrv = juvenile right valves; jc = juvenile carapaces; mni = minimum number of adult individuals; tv = total of adult plus juvenile valves.

Species	alv	arv	jlv	jrv	jc	mni	tv
Candona neglecta Sars, 1887	8	3	119	133	1	8 j	264
Cyprideis torosa (Jones, 1850)	10	9	2	7		10 j	28
Cypris pubera O.F.Müller, 1776			1	2		j	3
Ilyocypris bradyi Sars, 1890	3	1	5			3 j	9

Eight samples were devoid of fossil remains (empty circles in Fig. 4). One fossiliferous sample (CdT 230.80–230.90; full circle in Fig. 4) yielded an assemblage consisting of calcareous remains pertaining to mollusc (bivalve and gastropod) fragments and ostracod shells.

All of the ostracod remains (valves, carapaces and fragments, both adult specimens and young instars) were picked out and determined at specific level. The number of valves and number of specimens were counted. The number of valves included all juvenile and adult valves. The minimum number of individuals was calculated by adding the greater number between right and left adult valves to the number of adult carapaces. Four species in four genera were identified (Table 1).

Ostracod specimens show different states of preservation. *Candona neglecta* is represented by several juvenile shells pertaining to various developmental stages and rare, poorly preserved, adult valves. The species *Cypris pubera* occurs exclusively with very rare young instars. *Ilyocypris bradyi* adult valves are broken and darkened while juveniles are relatively well preserved. *Cyprideis torosa* is the sole species in a good state of preservation, whether adult or juvenile valves.

Palaeoecological interpretations are based on recent literature on non-marine ostracods (see Meisch, 2000 and references therein). The ostracod assemblage of the CdT 230.80–230.90 consists of three species presently living in continental waters plus the euryhaline ostracod *Cyprideis torosa*.

Ilyocypris bradyi and *Cypris pubera* are typical of shallow oligohaline (<4‰) flowing waters. We consider these species displaced from continental "freshwater" supply.

Candona neglecta tolerate mesohaline waters (<16‰). The dominance of juvenile specimens could indicate a palaeoenvironment where young instars were unable to reach the adult stage. Adult valves are probably displaced together with *Ilyocypris bradyi* and *Cypris pubera* remains. The well preserved specimens of *Cyprideis torosa* indicate a paralic palaeoenvironment under the influence of continental and marine waters. Importantly, no marine ostracod was found. The sediments are deposited in a coastal area, a few metres (or a few decimetres) above sea level, with mesohaline/polyhaline waters with a salinity value of about 20‰. The connection with the sea was probably restricted, not allowing the presence of euryhaline marine-brackish taxa.

3. Ground movement

The theory relating Quaternary glaciations to astronomical events was proposed by Milankovitch (1941) who explained how the three major orbital cycles induced a different insolation of the Earth, alternating cool and warm periods and the resulting advance and retreat of the polar ice caps. The corresponding sea level changes are dominated by a strongly asymmetric ~100 ka cyclicity: after progressive step-wise falling of the sea level (~80 ka) there followed a short, rapid and continuous sea level rise (~20 ka). Waelbroek et al. (2002) proposed a reconstruction of the RSL for the last climatic cycle, establishing robust regressions between RSL and benthic foraminifera oxygen isotopic ratios. This curve, and the associated confidence interval, appears to contain the many others proposed for this period, and is in line with that proposed by Lambeck et al. (2011) from the LGM and previously utilised by Marturano

et al. (2012) to analyse contemporaneous data reconsidered herein. For our study it is worth noting that during the cold period leading up to the LGM, rapid oscillations in sea level, with magnitude of tens of metres in time intervals of 1000 years or less, are superimposed on a gradually falling level, and also that the fall in sea level leading up to the LGM appears to have been as rapid as about 50 m in less than 1000 years (Lambeck et al., 2002). Prior to 40 kyr the average dating error is 1–4 kyr (Waelbroek et al., 2002). In Fig. 5 the sea level change of the last 80 kyr according to Waelbroek et al. (2002) is plotted together with the analysed fossiliferous sample at its present (P, 112 m b.s.l) and inferred depositional position (D, 48 m b.s.l., see below). Close to P we also show (cross-shaped) the depths of the marine deposits predating the CI recorded at the Trecase well (Brocchini et al., 2001). The same figure reports the time interval from the deposition of CI (39.5 ka) and older correlated deposits of the Campi Flegrei (CF, 58 ka). At the CdT borehole, the CF origin of most of the trachytic pyroclastic units older than the CI (CdT-f, CdT-g, CdT-h, CdT-i and CdT-j in Fig. 4), overlying the CdT-d and CdT-c deposits of uncertain provenance, is suggested both on the basis of lithological and sedimentological characteristics, and by the similarities of their Sr isotope compositions and geochemistry. In particular, these units prove to have been emplaced between 58 ± 3 and 44.3 ± 0.8 ka (Pappalardo et al., 1999; Di Renzo et al., 2007). Allowing for such correlations and the rapid oscillations of the sea level in this period, the age of deposition of the fossiliferous sample older than 58 ka is considered coincident with the nearest previous highstand at 60 kyr computed at 48 ± 15 m b.s.l. (D in Fig. 5). The lower CdT-a deposit (Fig. 4) originating in the Vesuvian area is possibly related to a previous relative lowstand around 65 ka.

Below we show that the choice of older sea levels would not change the underlying interpretation, but merely lead to variations in the computed value. The time trajectory of the fossiliferous deposit from the inferred and final position (line in Fig. 5) indicates a net subsidence of ~60 m at an apparent rate close to 1 mm/yr. This contrasts with the values recorded at Somma-Vesuvius from the last 20 kyr, which indicate an average uplift rate at least three times greater in absolute terms. Thus, in order to allow for the post LGM uplift, we should consider that the real trajectory (dashed line in Fig. 6) experiences a subsidence rate approaching ~3 mm/yr, at least three times higher than the average recorded on the plain for the last glacial cycle (Romano et al., 1994; Barra et al., 1991, 1992, 1996; Bellucci, 1998) and greater than the average 2 mm/yr estimated from the Lower Pleistocene (Ippolito et al., 1973). In sum, in the long term Mt. Somma-Vesuvius acts as a single structural element both experiencing uplift within the general subsidence framework of the Campanian Plain in the last 20 kyr and showing clear subsidence in the previous period.

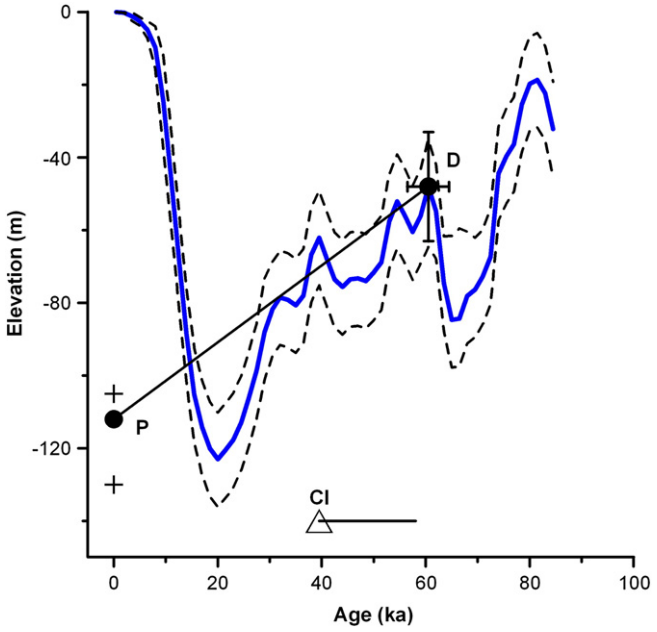

Fig. 5. Reconstruction of the ground movements at the CdT borehole site. The continuous curve represents the sea level change and the two dashed curves illustrate the upper and lower limits to the estimates (Waelbroek et al., 2002). The continuous line represents the relative ground movement from the inferred (D) to the present (P) position of the sample CdT 230.80–230.90. Crosses: marine deposits predating the CI at the Trecase well (Brocchini et al., 2001). On the bottom the time interval from the deposition of CI (39.5 ka) and older correlated deposits (58 ka) is also reported.

4. Volcano–tectonic inferences

One aim of this paper is to predate the knowledge of ground movements concerning Somma-Vesuvius, previously extended down to the LGM (Marturano et al., 2012), in order to infer on deep volcano–tectonic causes. Therefore it is essential to discriminate deformation due to magmatic processes and others that may also contribute, like regional tectonics and variable surface loading. These two quantities must be estimated and considered in the partition of the total vertical displacement.

Large-scale subsidence throughout the Campanian Plain was caused by sinking of the Mesozoic carbonate platform, which outcrops on the margin of the graben and is found at the depth of 1670 m under Somma-Vesuvius at the Trecase well (Brocchini et al., 2001). The plain is considered to be subsiding at an average rate of 0.6 ± 0.3 mm/yr from analysed sequences including Holocene and late Pleistocene deposits (Bellucci, 1998). Making due allowances for this average rate of subsidence, the vertical displacement of tectonic origin amounts to 60 ka to 36 ± 18 m.

Besides, crustal deformation at volcanoes may also be related to surface loading as well (Pinel et al., 2007). This is of particular interest during a cycle of edifice growth, in which the volume of the volcano varies considerably over a time span of kyears, eventually leading to elastic or isostatic crustal adjustments.

In the Somma-Vesuvius area, CI deposition was followed by local tuff cones, which predated the formation of the Mt. Somma edifice by extrusion of a thick sequence of lavas up to B eruption (22 ka) after which the activity became mainly explosive (Brocchini et al.,

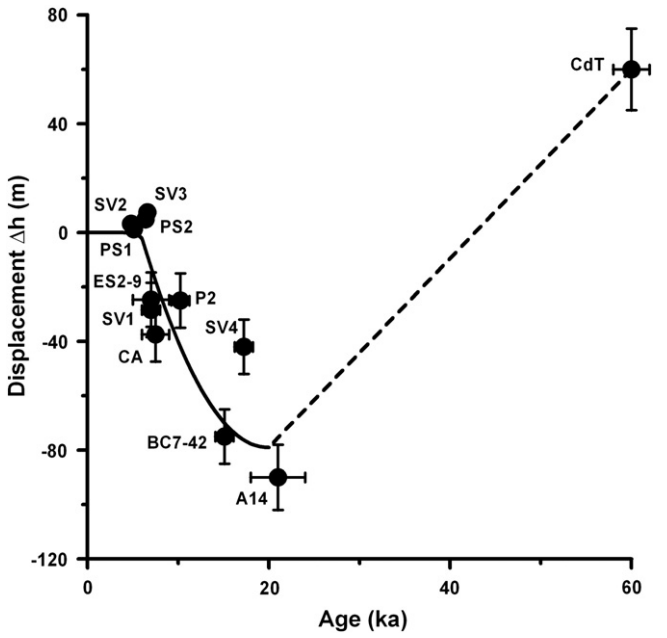

Fig. 6. Ground movement at Somma-Vesuvius in the last 60 kyr. CdT: Camaldoli della Torre site. Ground movement in the last 20 ka (continuous line: viscoelastic model) and data set (circles) as in Fig. 3.

2001; Di Renzo et al., 2007). This sequence may have been interrupted by the "Codola" plinian eruption occurring at 33 ka (Giaccio et al., 2008), the deposits of which occur in many medial to distal marine and terrestrial successions (e.g. Santacroce et al., 2008). At 22 ka, owing to the B eruption the calderisation of Mt. Somma began. Then a series of Holocene plinian eruptions (9 and 4.7 ka, AD 79) repeatedly collapsed the central part of the volcano built-up during the previous inter-plinian periods, modelling the caldera's present form. The recent cone, Vesuvius, grew within the caldera after the AD 79 "Pompeii" eruption. The caldera cuts a stratovolcano whose original summit can be placed from the present 1300 m up to 1600–1900 m elevation (see the two sections in Fig. 2) (Cioni et al., 1999). Therefore, in the cycle of edifice growth in the span of ~40 ka, from the palaeomarine level (60 ka) to eruption B (22 ka), the volcano varied its volume considerably, possibly leading to elastic and isostatic crustal adjustments. The deficiency of mass caused by ongoing calderisation induced by large eruptions (22, 9, 4.7 ka and AD 79) amounts to 1/40 of the total, proportionally contributing to the load-induced displacement calculated below.

Load-induced deformation on volcanoes is in general likely to be affected by a variation in rheology and crustal heterogeneities, and Maxwell viscoelastic behaviour with varying rheological parameters may be appropriate for the bulk of the crust. At Somma-Vesuvius local variations in crustal rheology remain poorly known, as do the fine details in load history for the last 60 ka.

An elastic half space and an elastic plate lying over ductile material can be considered two Earth model approximations, which may be used to calculate instantaneous and long-term surface displacements (Comer, 1983; Pinel et al., 2007). During the early stage of volcano growth, when the volcano's widths are small compared with the effective elastic part of the crust, the elastic half space is most applicable, bending deflections will be small and ground deformations will be due to local compression beneath the load. On a long time scale the elastic portion behaves like an elastic plate that bends in response to surface loads.

The volcanic edifice is believed to exist between two morphological extremes: a truncated cone 1100 m high, with base radius $r = 5000$ m, resembling the present shape, and a summit cone up to 1900 m with base radius of 1300 m, approaching the truncated part (~1 km^3), for a calculated total volume of 40 ± 1 km^3. The average density of the load is $\rho_m = 2200$ kg/m^3 (Berrino et al., 1998). The surface load before the initial stage of calderisation can be estimated around 30 MPa. For an elastic half-space with Poisson's ratio ν and Young's modulus E as elastic parameters, the vertical displacement of the surface induced by the distributed load of the stratovolcano can be calculated assuming that the entire weight of the volcano is evenly distributed over the base of a disc of density ρ and thickness h with the same total mass (e.g. Pinel and Jaupart, 2000). Poisson's ratio ν is assumed equal to 0.25. The dynamic Young's modulus for the underlying volcano-sedimentary fills can be estimated through the velocities of propagation of seismic waves (V_P and V_S). For the upper crust V_P is from 2.5 to 6.0 km/s and density ρ from 2.0 to 2.6 g/cm^3 (De Natale et al., 2004; Berrino et al., 1998). Assuming average density $\rho = 2.5$ g/cm^3, $V_P = 5.0$ km/s and $V_P/V_S = 1.8$, a value of $E \approx 50$ GPa is obtained. The value of Young's modulus mainly influences the amplitude of the displacement: a minimum for E gives us a maximum estimate of the displacement. Here a static value of Young's modulus should be used, which is at least half as low as the dynamic value, if not even one order lower (Gudmundsson, 1988; Wallmann et al., 1988; Pinel and Jaupart, 2004).

For $E = 30$–40 GPa the vertical displacement is 2–3 m and 20–30 m at the well location for the elastic and completely relaxed state respectively. A factor of 10 between the two end-members is corroborated by theoretical and field experiments (Comer, 1983; Pinel et al., 2007). In sum, an amount of about 25 ± 5 m may be reasonably imputed at the borehole location. The two ground movements connected to tectonic and loading causes ($36 + 25 = 61 \pm 23$ m) must be subtracted from the subsidence value detected by the CdT sample in order to obtain the volcanotectonic contribution. In Fig. 7 the corrected value is reported with the total error estimated (CdT-C). Finally, the 60 kyr vertical component of displacement involving the volcano (CdT elevation in Fig. 7) appears quasi-entirely due to tectonic (subsidence of the Campanian Plain) and loading effects, indicating substantial volcano–tectonic stability (CdT-C close to $\Delta H = 0$ in Fig. 7).

5. Discussion

The ground movements concerning Somma-Vesuvius since the LGM have been described elsewhere (Marturano et al., 2009, 2011, 2012). Synchronous uplift involving Herculaneum and Pompeii, the Sebeto and Sarno Plains, on the opposite sides of the volcano, has raised the whole Somma-Vesuvius structural block by several tens of metres during the last 20 ka. As an indication, Holocene marine deposits have been recovered today up to 25 m a.s.l. (above sea level). An axisymmetric deep source of strain was considered responsible for the long-term uplift, emphasising the role of magmatic movements (Marturano et al., 2012). These authors did not apply load corrections to the data throughout the period examined, since the form of the volcano did not significantly vary. Further, regional tectonics, a factor >3 slower than the uplift rate, was regarded only as a possible bias but not explicitly considered. Here data 2–3 times more remote reveal that the area may have been affected by several sources of strain: by considerable load changes, for a certain time (60 to 20 ka), and by regional tectonics, throughout the period (60 ka). Such ground-induced deformations can mistakenly be interpreted in the study of the volcano–tectonic process. Fig. 5 shows that, on average, the Somma-Vesuvius block subsided (line D–P) in the last 60 ka, differing from the uplift recorded in the last 20 ka (Fig. 3). The real ground

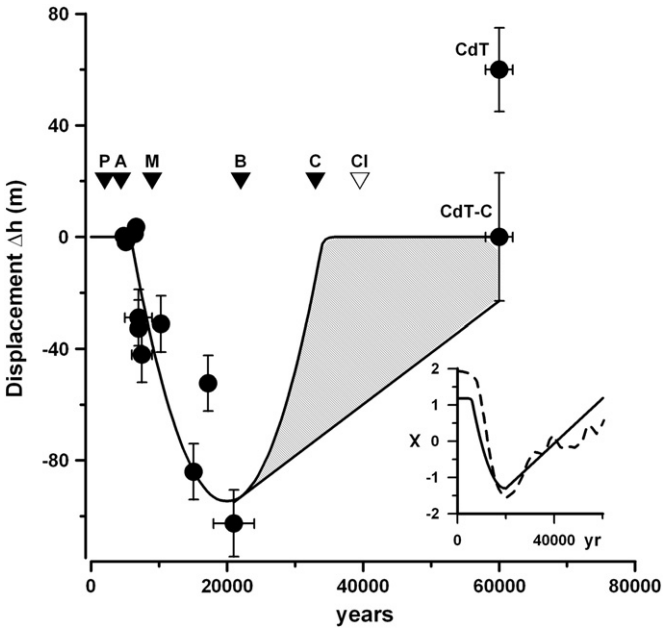

Fig. 7. Volcano–tectonic ground movement history at Somma-Vesuvius in the last 60 ka. Ground movement and data set as in Fig. 6 corrected by regional tectonic and loading effect; $|\Delta h_{max}| = 92$ m (Cfr with Figs. 3 and 6). CdT-C represents the corrected position of CdT. The dashed area from 60 to 20 kyr represents the region within which possible movement trajectories can be found. The plinian eruptions of the Somma-Vesuvius are reported (filled triangles). The empty triangle represents the CI eruption. Inset: normalised time evolution curves of sea-level change (dashed) and ground deformations at Somma-Vesuvius (continuous) in the last 60 ka; the residuals from the mean are normalised by their standard deviation; on the vertical axis $X = (N-\sigma)/\delta$; σ = mean; δ = stand. dev.

movements are represented in Fig. 6. As suggested by geological and physical models (Patacca et al., 1990; Luongo et al., 1991) and supported by strain rate measurements (Barra et al., 1991, 1992; Romano et al., 1994; Bellucci, 1998), the Campanian Plain subsided throughout the last glacial cycle (125 ka). Also, the form of the volcano, from the initial stage of its subaerial phase, here fixed at 60 ka, varied significantly until 20 ka, growing in size possibly up to 1900 m in height (Brocchini et al., 2001; Di Renzo et al., 2007; Cioni et al., 2008). In order to separate the single contributions, regional tectonics and loading were estimated and subtracted from the experimental results.

The complete data set of the ground movements detected at Somma-Vesuvius [i.e., those of Marturano et al. (2012), here corrected by regional tectonic trend and loading effects, and the present data] is illustrated in Fig. 7. The data for the last 20 ka appear indicating ground uplift, connected to volcano–tectonic process, for the whole period. The finding of a fossiliferous layer indicates an inversion of the movement (Figs. 6 and 7). While the large error does not ensure a narrow choice in time, a turning point is possibly marked around the LGM. By considering the errors, the continuous lines (Fig. 7) describe a region within which possible trajectories originated by the volcano–tectonic process can be found. The higher rate of subsidence (the left border of the region) is in symmetry with the post-LGM uplift.

For glaciated regions, glaciations and eruption rates have been correlated, taking account of the loading effect both on magma generation and on storage conditions (Gudmundsson, 1986; Jull and McKenzie, 1996; Sigvaldason et al., 1992; Jellinek et al., 2004; Geyer and Bindeman, 2011).

The period considered here extends for one half of the last glacial cycle in which the tensile stress change associated with glaciation–deglaciation may be an important trigger for volcanism away from the ice loads where the crust reaction is sensitive to the visco-elastic response caused by meltwater loading history (Sparks et al., 1977; Rampino et al., 1979; Wallmann et al., 1988; Nakada and Yokose, 1992). As regards the study area, it has been suggested that periodic occurrence of eruptions is controlled by change in glacio-eustatic pressure (Paterne and Guichard, 1993; McGuire et al., 1997). The results presented here can be directly associated to deep (lower crust–mantle boundary) mass movements occurring in the long term. Rheological and material interfaces (such as the Moho or the brittle–ductile transition) provide a natural initial density trap for rising magmas (e.g., Watanabe et al., 1999). The magma system of Somma-Vesuvius was modelled bearing this picture in mind.

From our analysis, the hinge point separating different ground deformation styles (subsidence to uplift) can be placed around the LGM. The data regarding sea-level change and ground deformations at Somma-Vesuvius indicate clear relationships between the two phenomena (inset in Fig. 7): a fascinating relation proposed over half a century ago about the tectonic implications of ocean and lake unloading on volcanoes (Thorarinsson, 1953; Matthews, 1969).

Bearing in mind that only large eruptions (Volcanic Explosivity Index, VEI ≥ 5), albeit relatively rare events, can be representative of the volcano cyclic activity over the long time scales analysed here, there remain many critical questions which are both scientific and related to minimising the associated risks. Why, for example, did the largest eruptions apparently occur at the extreme values of ground deformations and at 12 ± 1 and 3 ± 1 kyr typical time lags? Also, is the present repose time an inter-plinian interval or will the next eruption change in magnitude or style? Geological records reveal that Somma-Vesuvius is sensitive to global change and that it is cadenced by plinian eruptions, involving the whole plumbing system and surface areas beyond the edifice itself. Studies of a single plinian eruption, like the last one in AD 79, seem to confirm the pattern of deformation together with clear precursor signals on a large scale (Marturano, 2008). Despite the apparent complexity of individual volcanic eruptions, the physical processes which govern them are often surprisingly simple (Parfitt and Wilson, 2008).

Acknowledgements

We are grateful to M. Di Vito for allowing analysis of the core samples and making useful comments during the earliest stages of the work. We would like to thank L. Ferranti and L. Pappalardo for helpful specialist discussions. Comments and suggestions from M. Battaglia and two anonymous reviewers greatly helped to improve the manuscript. The authors also thank the Editor L. Wilson.

References

Barra, D., Cinque, A., Gewelt, M., Hurtgen, C., 1991. L'ospite caldo *Sylvestra seminis* (Bonaduce, Masoli & Pugliese, 1976) (Crustacea, Ostracoda): un possibile marker dell'ultimo interglaciale dell'area mediterranea. Il Quaternario 4, 327–332.

Barra, D., Bonaduce, G., Brancaccio, L., Cinque, A., Ortolani, F., Pagliuca, S., Russo, F., 1992. Evoluzione geologica olocenica della piana costiera del Fiume Sarno (Campania). Memorie della Societa Geologica Italiana 42, 255–267.

Barra, D., Romano, P., Santo, A., Campajola, L., Roca, V., Tuniz, C., 1996. The Versilian transgression in the Volturno River Plain (Campania, Southern Italy): palaeoenvironmental history and chronological data. Il Quaternario 9 (2), 445–458.

Bellucci, F., 1998. Nuove conoscenze stratigrafiche sui depositi effusivi ed esplosivi nel sottosuolo dell'area del Somma-Vesuvio. Bollettino della Societa Geologica Italiana 117, 385–405.

Berrino, G., Corrado, G., Riccardi, U., 1998. Sea gravity data in the Gulf of Naples: a contribution to delineating the structural pattern of the Vesuvian area. Journal of Volcanology and Geothermal Research 82, 139–150.

Bonafede, M., Dragoni, M., Quareni, F., 1986. Displacement and stress fields produced by a centre of dilation and by a pressure source in a viscoelastic half-space: application to the study of ground deformation and seismic activity at Campi Flegrei, Italy. Geophysical Journal of the Royal Astronomical Society 87, 455–485.

Borgia, A., Tizzani, P., Solaro, G., Manzo, M., Casu, F., Luongo, G., Pepe, A., Berardino, P., Fornaro, G., Sansosti, E., Ricciardi, G.P., Fusi, N., Di Donna, G., Lanari, R., 2005. Volcanic spreading of Vesuvius, a new paradigm for interpreting its volcanic activity. Geophysical Research Letters 32, L03303. http://dx.doi.org/10.1029/2004GL022155.

Brocchini, D., Principe, C., Castradori, D., Laurenzi, M.A., Gorla, L., 2001. Quaternary evolution of the southern sector of the Campanian Plain and early Somma-Vesuvius activity: insights from the Trecase I well. Mineralogy and Petrology 73, 67–91.

Cioni, R., Santacroce, R., Sbrana, A., 1999. Pyroclastic deposits as a guide for reconstructing the multi-stage evolution of the Somma-Vesuvius Caldera. Bulletin of Volcanology 61, 207–222.

Cioni, R., Longo, A., Macedonio, G., Santacroce, R., Sbrana, A., Sulpizio, R., Andronico, D., 2003. Assessing pyroclastic fall hazard through field data and numerical simulations: example from Vesuvius. Journal of Geophysical Research 108 (B2). http://dx.doi.org/10.1029/2001JB000642.

Cioni, R., Bertagnini, A., Santacroce, R., Andronico, D., 2008. Explosive activity and eruption scenarios at Somma-Vesuvius (Italy): towards a new classification scheme. Journal of Volcanology and Geothermal Research 178, 331–345. http://dx.doi.org/10.1016/j.jvolgeores.2008.04.024.

Comer, P.R., 1983. Thick plate flexure. Geophysical Journal of the Royal Astronomical Society 72, 101–113.

Costa, A., Folch, A., Macedonio, G., Giaccio, B., Isaia, R., Smith, V.C., 2012. Quantifying volcanic ash dispersal and impact of the Campanian Ignimbrite supereruption. Geophysical Research Letters 39, L10310. http://dx.doi.org/10.1029/2012GL051605.

Dalla Via, G., Sabatini, R., De Natale, G., Pingue, F., 2005. Lithospheric rheology in southern Italy inferred from post seismic viscoelastic relaxation following the 1980 Irpinia earthquake. Journal of Geophysical Research 110, B06311. http://dx.doi.org/10.1029/2004JB003539.

De Natale, G., Chiarabba, C., Troise, C., Trigila, R., Dolfi, D., Kissling, E., 2004. Seismicity and 3D sub-structure at Somma-Vesuvius volcano: evidence for magma quenching due to H_2O exolution. Earth and Planetary Science Letters 221, 181–196.

De Natale, G., Troise, C., Pingue, F., Mastrolorenzo, G., Pappalardo, L., 2006. The Somma-Vesuvius volcano (Southern Italy): structure, dynamics and hazard evaluation. Earth-Science Reviews 74, 73–111.

De Vivo, B., Rolandi, G., Gans, P.B., Calvert, A., Bohrson, W.A., Spera, F.J., Belkin, H.E., 2001. New constraints on the pyroclastic eruptive history of the Campanian Volcanic Plain (Italy). Mineralogy and Petrology 73, 47–65.

Di Renzo, V., Di Vito, M.A., Arienzo, I., Carandente, A., Civetta, L., D'antonio, M., Giordano, F., Orsi, G., Tonarini, S., 2007. Magmatic history of Somma-Vesuvius on the basis of new geochemical and isotopic data from a deep borehole (Camaldoli della Torre). Journal of Petrology 48, 753–784.

Fedele, L., Scarpati, C., Lanphere, M., Melluso, L., Morra, V., Perrotta, A., Ricci, G., 2008. The Breccia Museo formation, Campi Flegrei, southern Italy: geochronology, chemostratigraphy and relationship with the Campanian Ignimbrite eruption. Bulletin of Volcanology 70, 1189–1219.

Geyer, A., Bindeman, I., 2011. Glacial influence on caldera-forming eruptions. Journal of Volcanology and Geothermal Research 202, 127–142.

Giaccio, B., Isaia, R., Fedele, F.G., Di Canzio, E., Hoffecker, J., Ronchitelli, A., Sinitsyn, A.A., Anikovich, M., Lisitsyn, S.N., Popov, V.V., 2008. The Campanian Ignimbrite and Codola tephra layers: two temporal/stratigraphic markers for the Early Upper

Palaeolithic in southern Italy and eastern Europe. Journal of Volcanology and Geothermal Research 177, 208–226.
Gordon, R.G., Stein, S., DeMets, C., Argus, D.A., 1987. Statistical tests for closure of plate motion circuits. Geophysical Research Letters 14, 587–590.
Gudmundsson, A., 1986. Mechanical aspects of postglacial volcanism and tectonics of the Reykjanes Peninsula, southwest Iceland. Journal of Geophysical Research 91, 12711–12721.
Gudmundsson, A., 1988. Effect of tensile stress concentration around magma chambers on intrusion and extrusion frequencies. Journal of Volcanology and Geothermal Research 35, 179–194.
Ippolito, F., Ortolani, F., Russo, M., 1973. Struttura marginale tirrenica dell'Appennino campano: reinterpretazione di dati di antiche ricerche di idrocarburi. Memorie della Societa Geologica Italiana 12, 127–250.
Jellinek, A.M., Manga, M., Saar, M.O., 2004. Did melting glaciers cause volcanic eruptions in eastern California? Probing the mechanics of dike formation. Journal of Geophysical Research 109, B09206. http://dx.doi.org/10.1029/2004JB002978.
Joron, J.L., Metrich, N., Rosi, M., Santacroce, R., Sbrana, A., 1987. In: Santacroce, R. (Ed.), Chemistry and petrography: Somma-Vesuvius. C.N.R.: Quaderni de 'La Ricerca Scientifica', 114, pp. 105–174 (Rome).
Jull, M., McKenzie, D., 1996. The effect of deglaciation on the mantle melting beneath Iceland. Journal of Geophysical Research 101, 21815–21828.
Karlstrom, L., Dufek, J., Manga, M., 2010. Magma chamber stability in arc and continental crust. Journal of Volcanology and Geothermal Research 190, 249–270.
Lambeck, K., Yokoyama, Y., Purcell, T., 2002. Into and out of the Last Glacial Maximum: sea-level change during oxygen isotope stages 3 and 2. Quaternary Science Reviews 21, 343–360.
Lambeck, K., Antonioli, F., Anzidei, M., Ferranti, L., Leoni, G., Scicchitano, G., Silenzi, S., 2011. Sea level change along the Italian coast during the Holocene and projections for the future. Quaternary International 232, 250–257. http://dx.doi.org/10.1016/j.quaint.2010.04.026.
Luongo, G., Cubellis, E., Obrizzo, F., Petrazzuoli, S.M., 1991. A physical model for the origin of volcanism of the Tyrrhenian margin: the case of the Neapolitan area. Journal of Volcanology and Geothermal Research 48, 173–185.
Marturano, A., 2008. Sources of ground movements of Vesuvius before the AD 79 eruption: evidence from contemporary accounts and archaeological studies. Journal of Volcanology and Geothermal Research 177, 959–970.
Marturano, A., Aiello, G., Barra, D., Fedele, L., Grifa, C., Morra, V., Berg, R., Varone, A., 2009. Evidence for Holocenic uplift at Somma-Vesuvius. Journal of Volcanology and Geothermal Research 184, 451–461.
Marturano, A., Aiello, G., Barra, D., 2011. Evidence for Late Pleistocene uplift at the Somma-Vesuvius apron near Pompeii. Journal of Volcanology and Geothermal Research 202, 211–227. http://dx.doi.org/10.1016/j.jvolgeores.2011.02.010.
Marturano, M., Aiello, G., Barra, D., Fedele, L., Morra, V., 2012. Ground movement at Somma-Vesuvius from Last Glacial Maximum. Journal of Volcanology and Geothermal Research 211–212, 24–35.
Matthews, R.K., 1969. Tectonic implications of glacio-eustatic sea level fluctuations. Earth and Planetary Science Letters 5, 459–462.
McGuire, W., Howard, R., Firth, C., Solow, A., Pullen, A., Saunders, S., Stewart, I., Vita-Finzi, C., 1997. Correlation between rate of sea level and frequency of explosive volcanism in the Mediterranean. Nature 389, 473–476.
Meisch, C., 2000. In: Schwoerbel, J., Zwick, P. (Eds.), Freshwater Ostracoda of Western and Central Europe, 8/3. Spektrum Academischer Verlag, Heidelberg, Germany (522 pp.).
Milankovitch, M., 1941. Kanon der Erdbestrahlung und seine Anwendung auf das Eiszeitenproblem. Royal Serbian Academy Special Publication, 133 (633 pp.).
Nakada, M., Yokose, H., 1992. Ice age as a trigger of active Quaternary volcanism and tectonism. Tectonophysics 212, 321–329.
Nooner, S.L., Bennati, L., Calais, E., Buck, W.R., Hamling, I.J., Wright, T.J., Lewi, E., 2009. Post-rifting relaxation in the Afar region Ethiopia. Geophysical Research Letters 36, L21308. http://dx.doi.org/10.1029/2009GL040502.
Nunziata, C., Natale, M., Luongo, G., Panza, F.G., 2006. Magma reservoir at Mt. Vesuvius: size of the hot, partially molten, crust material detected deeper than 8 km. Earth and Planetary Science Letters 242, 51–57.
Okada, Y., 1992. Internal deformation due to shear and tensile faults in a half-space. Bulletin of the Seismological Society of America 82, 1018–1040.
Panza, G.P., Peccerillo, A., Aoudia, A., Farina, B., 2007. Geophysical and petrological modelling of the structure and composition of the crust and upper mantle in complex geodynamic settings: the Tyrrhenian Sea and surroundings. Earth-Science Reviews 80, 1–46.
Pappalardo, L., Civetta, L., D'Antonio, M., Deino, A., Di Vito, M.A., Orsi, G., Carandente, A., de Vita, S., Isaia, R., Piochi, M., 1999. Chemical and Sr-isotopical evolution of the Phlegrean magmatic system before the Campanian Ignimbrite (37 ka) and the Neapolitan Yellow Tuff (12 ka) eruptions. Journal of Volcanology and Geothermal Research 91, 141–166.
Parfitt, E.A., Wilson, L., 2008. Fundamentals of Physical Volcanology. Blackwell (230 pp.).
Patacca, E., Sartori, R., Scandone, P., 1990. Tyrrhenian basin and apenninic arcs: kinematic relations since late Tortonian times. Memorie della Società Geologica Italiana 45, 425–451.
Paterne, M., Guichard, F., 1993. Triggering of volcanic pulses in the Campanian area, South Italy, by periodic deep magma influx. Journal of Geophysical Research 98, 1861–1873.
Pinel, V., Jaupart, C., 2000. The effect of edifice load on magma ascent beneath a volcano. Philosophical Transactions. Royal Society of London A 358, 1515–1532.
Pinel, V., Jaupart, C., 2004. Magma storage and horizontal dyke injection beneath a volcanic edifice. Earth and Planetary Science Letters 221, 245–262. http://dx.doi.org/10.1016/j.epsl.2004.01.031.
Pinel, V., Sigmundsson, F., Sturkell, E., Geirsson, H., Einarsson, P., Gudmundsson, M.T., Högnadòttir, T., 2007. Discriminating volcano deformation due to magma movements and variable surface loads: application to Katla subglacial volcano. Icelandic of Geophysical Journal International 169, 325–338.
Rampino, M.R., Self, S., Fairbridge, R.W., 1979. Can rapid climatic change cause volcanic eruptions? Science 206, 826–829.
Romano, P., Santo, A., Voltaggio, M., 1994. L'evoluzione geomorfologica della Pianura del Fiume Volturno (Campania) durante il tardo Quaternario (Pleistocene medio-Superiore-Olocene). Il Quaternario 7, 41–56.
Santacroce, R., 1987. Somma-Vesuvius. CNR Quaderni de "La Ricerca Scientifica" 114 (8), 251.
Santacroce, R., Cioni, R., Marianelli, P., Sbrana, A., Sulpizio, R., Zanchetta, G., Donahue, D.J., Joron, J.L., 2008. Age and whole rock–glass compositions of proximal pyroclastics from the major explosive eruptions of Somma-Vesuvius: a review as a tool for distal tephrostratigraphy. Journal of Volcanology and Geothermal Research 177, 1–18.
Scaillet, B., Pichavant, M., Cioni, R., 2008. Upward migration of Vesuvius magma chamber over the past 20,000 years. Nature 455, 216–220. http://dx.doi.org/10.1038/nature07232.
Sigvaldason, G.E., Annertz, K., Nielsson, M., 1992. Effect of glacier loading/deloading on volcanism: postglacial volcanic production rate of the Dyngjufjöll area, central Iceland. Bulletin of Volcanology 54, 385–392.
Sparks, S.R.J., Sigurdsson, H., Wilson, L., 1977. Magma mixing: a mechanism for triggering acid explosive eruptions. Nature 267, 315–318.
Thorarinsson, S., 1953. Some new aspects of the Grímsvötn problem. Journal of Glaciology 2 (14), 267–276.
Waelbroek, C., Labeyrie, L., Michel, E., Duplessy, J.C., Mc Manus, J.F., Lambeck, K., Balbon, E., Labracherie, M., 2002. Sea level and deep water temperature changes derived from benthic foraminifera isotopic records. Quaternary Science Reviews 21, 295–305.
Wallmann, P.C., Mahood, G.A., Pollard, D.D., 1988. Mechanical models for correlation of ring-fracture eruptions at Pantelleria, Straits of Sicily, with glacial sea-level drawdown. Bulletin of Volcanology 50, 327–339.
Watanabe, T., Koyaguchi, T., Seno, T., 1999. Tectonic stress controls on ascent and emplacement of magmas. Journal of Volcanology and Geothermal Research 91, 65–78.
Zollo, A., Gasparini, P., Virieux, J., Biella, G., Boschi, E., Capuano, P., de Franco, R., Dell'Aversana, P., De Matteis, R., De Natale, G., Iannaccone, G., Guerra, I., Le Meur, H., Mirabile, L., 1998. An image of Mt. Vesuvius obtained by 2D seismic tomography. Journal of Volcanology and Geothermal Research 82, 161–173.